

### *Supporting Methods*

The initial coordinates used in these computational studies were taken from the 2.0Å crystal structure of the TS ribozyme<sup>1</sup> (PDB 5T5A). All simulations were performed with the AMBER14 package;<sup>2</sup> using `rism1d` and `rism3d.snglpnt` for the 3D-RISM<sup>3</sup> calculations and `pmemd.cuda`<sup>4</sup> for the molecular dynamics simulations. For each of the simulations, the ribozyme was solvated in a truncated octahedral box with a 15.0Å buffer of TIP4P-Ew<sup>5</sup> waters and 140mM NaCl. The AMBER ff14SB force field<sup>6</sup> was used, with monovalent and divalent ion parameters designed for use with the TIP4P-Ew water model.<sup>7,8</sup> Prior to production runs of the molecular dynamics simulations all structures were subjected to 10ns of solvent annealing and solute equilibration, with the details of this procedure previously described in the ribozyme literature.<sup>9</sup>

For the 3D-RISM calculation of the crystallographic coordinates, the missing hydrogen atoms were added in using LEAP and the metal ions were removed. The solution structure was taken from the end of the aforementioned equilibration procedure and was stripped of all solvent and metal ions prior to the 3D-RISM calculations. The initial 1D solvent susceptibility was calculated using SPC/E water<sup>10</sup> with Na<sup>+</sup> and Cl<sup>-</sup> ions with concentrations of 55.5M, 140mM, and 140mM respectively. The 3D-RISM calculations were solved with both the crystallographic and solution structure aligned to the same 142 by 156 by 110Å grid with gridpoints spaced every 0.5Å, such that a difference map between the two calculations could be constructed from the cation number density.

In order to explore potential rearrangements from the crystallographic structure to an active conformation in solution, the O2' nucleophile was modeled in and covalently bonded to the scissile phosphate making a pentacoordinate phosphorane transition state mimic. First, a 100 ns simulation of a transition state mimic starting from the crystallographic coordinates for the RNA and Mg<sup>2+</sup> ions was completed. Guided by the results from the 3D-RISM calculations, the Mg<sup>2+</sup> ion at the M4 site in the both crystal structure and previous simulation was moved to the Watson-Crick edge of C7 (M4' site) and restrained to directly coordinate the N3 of that residue. An additional restraint was applied to bring the O5' leaving group within outer-sphere coordination distance

(5Å) of the  $\text{Mg}^{2+}$ , consistent with the hypothesized model that a  $\text{Mg}^{2+}$  bound water could act as the general acid. Three independent trajectories (different starting velocities) were propagated for 20 ns with statistics being calculated from the final 10 ns. From these simulations where the spontaneous rearrangement of the active site was observed, the two proposed computational models were developed. For the "Mg Acid" model, an additional 25 ns of molecular dynamics was carried out with the sole restraint keeping the  $\text{Mg}^{2+}$  (presumed to act as the general base) outer-sphere coordinated to the N3 of A9.

The "C7 Acid" model was developed by starting with the structure observed in the simulation where a  $\text{Mg}^{2+}$  at C7 induced the rearrangement of the active site. This  $\text{Mg}^{2+}$  was returned to the crystallographic M4 site, while C7 was protonated at the N3 position. Additionally, U57 was deleted (a mutation shown to have minimal effect on the rate)<sup>1</sup> as a means to reduce the conformational sample space. Following roughly 10 ns of equilibration where C7:N3H<sup>+</sup> was restrained to hydrogen bond with the O5' leaving group, all restraints were slowly removed and 50 ns of unrestrained dynamics were performed. A second 25 ns long trajectory with a restraint keeping the general base  $\text{Mg}^{2+}$  within 5Å of A9:N3 was completed in order to focus in on conformations that would be representative of the ribozyme at the transition state.

The "Mg Acid" and "C7 Acid" models provided here as supplementary datasets 1 and 2, respectively, are the average structures from the two 25 ns trajectories with the presumptive general base  $\text{Mg}^{2+}$  restrained to within 5Å of A9:N3. These two average structures were then used in the 3D-RISM calculations confirming the positioning of the active site  $\text{Mg}^{2+}$  ions seen in the MD trajectories (Figures S4 and S5).

*Supplementary Figures*

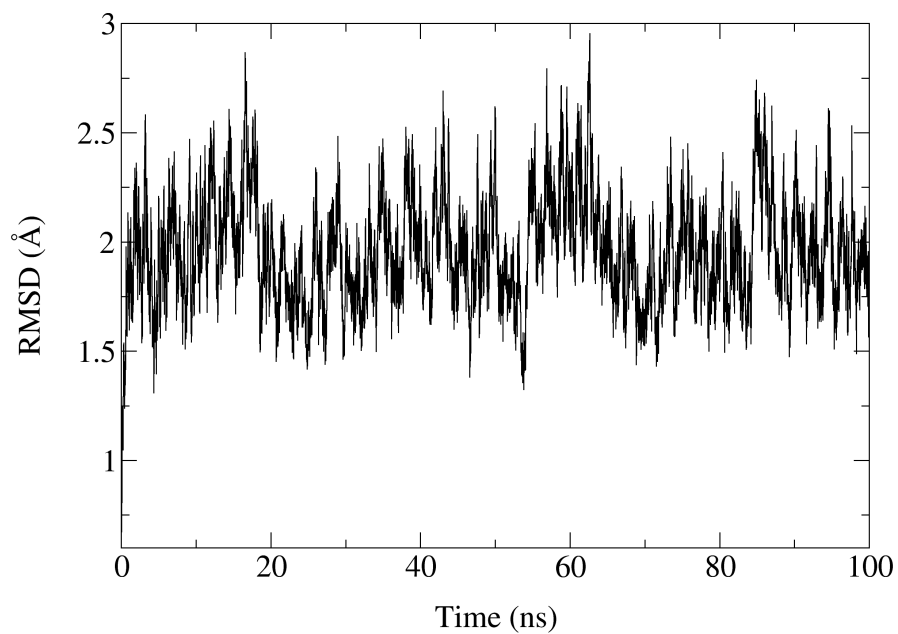


Figure S1: Time series of the best-fit heavy atom RMSD for an unrestrained 100 ns of the TSrz starting from the crystallographic coordinates for all RNA and  $Mg^{2+}$  ions. Additionally, C54:O2' was modeled in as part of pentacoordinate phosphorane transition state mimic. Snapshots were taken every 10 ps and aligned to the crystallographic coordinates deposited in the Protein Data Bank as PDB ID: 5T5A<sup>1</sup>

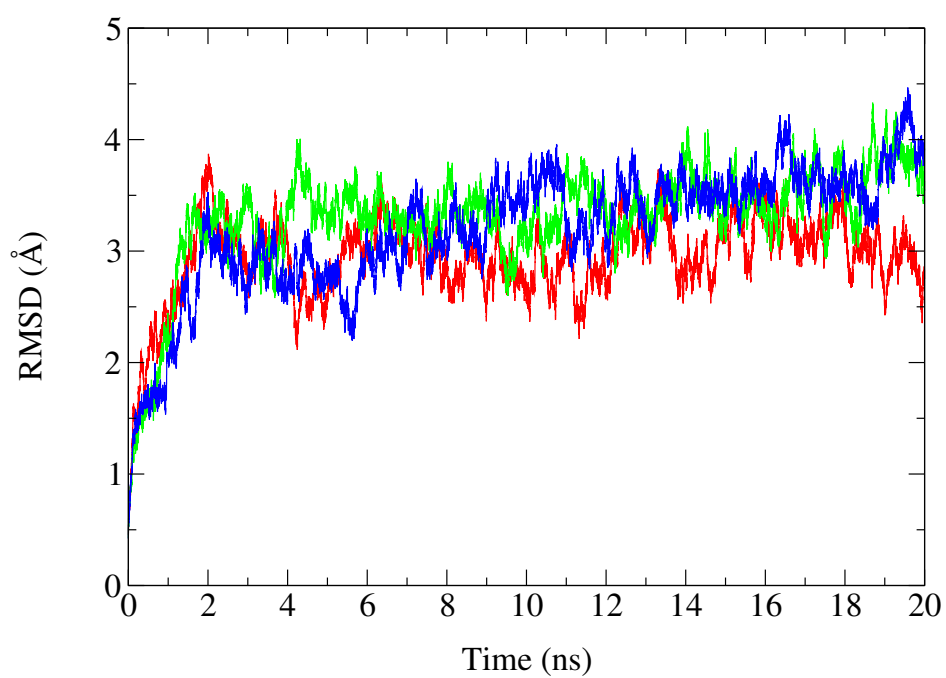


Figure S2: Time series of the best-fit heavy atom RMSD from the three independent trajectories (same initial coordinates, but different starting velocities) where a  $\text{Mg}^{2+}$  ion at the M4' site induced a spontaneous rearrangement of the TSrz active site.

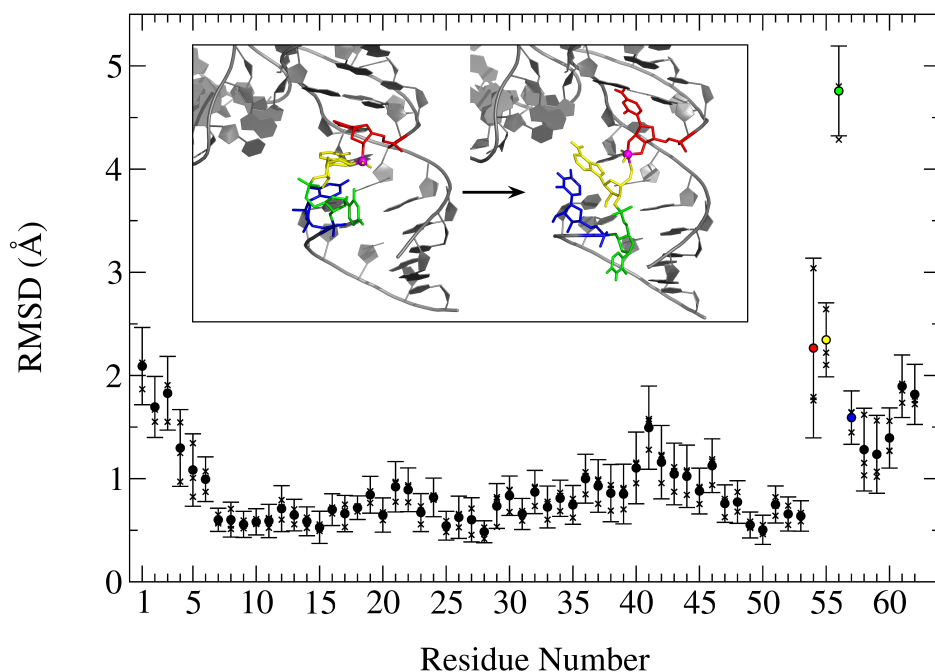


Figure S3: Average per residue RMSD (and standard deviation) from the final 10 ns of the simulation trajectory where a  $\text{Mg}^{2+}$  ion at the M4' site induced a spontaneous rearrangement of the TSrz active site (Figure S2). The reference structure, to which all residues were aligned and the RMSD was calculated, is the structure corresponding to the end of an equilibration run where the crystallographic coordinates relax to the inclusion of the transition state mimic phosphorane. Residues 54 - 57 are highlighted with the colors used for the corresponding residues in the inset figure. Inset: Rearrangement of the TSrz active site following the placement of a  $\text{Mg}^{2+}$  ion at the M4' site. Residues C54, A55, U56, and U57 (the residues that experience the significant rearrangement) are represented as sticks and highlighted in red, yellow, green, and blue, respectively. The scissile phosphate is highlighted as a magenta sphere. Inset left: Crystallographic structure PDB ID: 5T5A.<sup>1</sup> Inset right: Average structure from the final 10 ns of the three "rearrangement" trajectories combined.

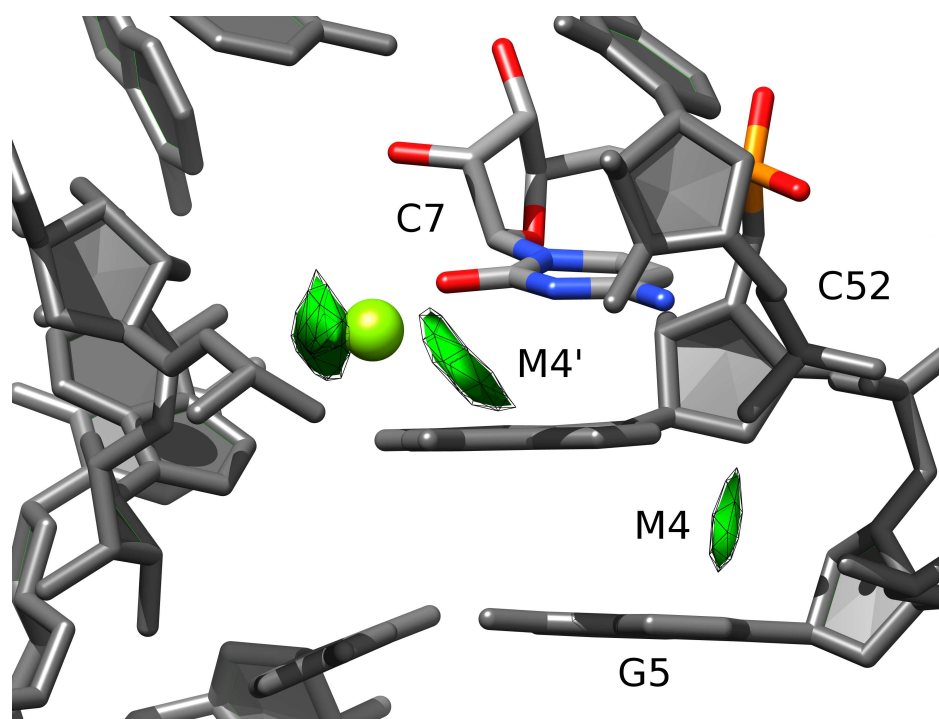


Figure S4: Cation density around C7 predicted by 3D-RISM for the "Mg Acid" model overlaid on the average structure from a 25 ns MD trajectory with the presumptive general base restrained. There is significant density at both the M4 and M4' sites, with the higher predicted fractional occupancy at the M4' site. The C7 residue is highlighted in color and a stick representation, while the Mg<sup>2+</sup> ion is shown as a green sphere.

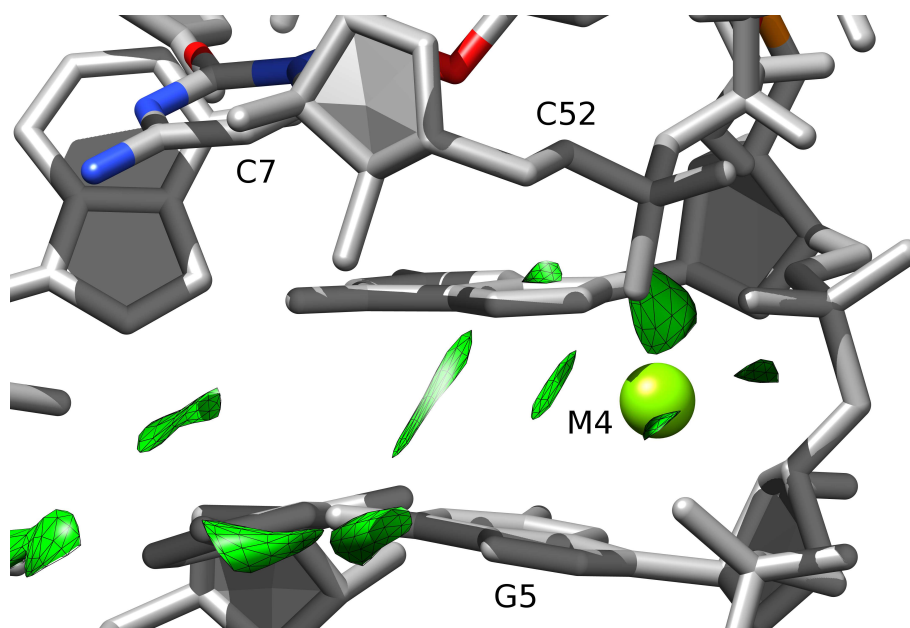


Figure S5: Predicted cation density from the 3D-RISM, using the average structure from a 25 ns simulation of the "C7 acid" model. Cation density is centered around the crystallographically observed M4 site. While no density was predicted directly at the M4 Mg<sup>2+</sup> ion, this is likely due to 3D-RISM not being able to place cations in the small space available between the non-bridging phosphoryl oxygens of C52 and G5 tightly bound to the Mg<sup>2+</sup> ion (Note: The Mg<sup>2+</sup> ions are stripped from the coordinate file, and the 3D-RISM calculation is run without additional relaxation or rearrangement of the RNA structure). The C7 residue is highlighted in color and a stick representation, while the Mg<sup>2+</sup> ion is shown as a green sphere.

## References

- (1) Liu, Y.; Wilson, T. J.; Lilley, D. M. J. *Nat. Chem. Biol.* **2017**, *13*, 508–513.
- (2) Case, D. A.; Babin, V.; Berryman, J. T.; Betz, R. M.; Cai, Q.; Cerutti, D.; Cheatham III, T. E.; Darden, T. A.; Duke, R. E.; Gohlke, H.; Götz, A. W.; Gusarov, S.; Homeyer, N.; Janowski, P.; Kaus, J.; Kolossváry, I.; Kovalenko, A.; Lee, T.; Le Grand, S.; Luchko, T.; Luo, R.; Madej, B.; Merz, K. M.; Paesani, F.; Roe, D. R.; Roitberg, A.; Sagui, C.; Salomon-Ferrer, R.; Seabra, G.; Simmerling, C. L.; Smith, W.; Swails, J.; Walker, R. C.; Wang, J.; Wolf, R. M.; Wu, X.; Kollman, P. A. AMBER 14. University of California, San Francisco: San Francisco, CA, 2014.
- (3) Luchko, T.; Gusarov, S.; Roe, D. R.; Simmerling, C.; Case, D. A.; Tuszynski, J.; Kovalenko, A. *J. Chem. Theory Comput.* **2010**, *6*, 607–624.
- (4) Salomon-Ferrer, R.; Götz, A. W.; Poole, D.; Le Grand, S.; Walker, R. C. *J. Chem. Theory Comput.* **2013**, *9*, 3878–3888.
- (5) Horn, H. W.; Swope, W. C.; Pitner, J. W.; Madura, J. D.; Dick, T. J.; Hura, G. L.; Head-Gordon, T. *J. Chem. Phys.* **2004**, *120*, 9665–9678.
- (6) Maier, J. A.; Martinez, C.; Kasavajhala, K.; Wickstrom, L.; Hauser, K. E.; Simmerling, C. *J. Chem. Theory Comput.* **2015**, *11*, 3696–3713.
- (7) Joung, I. S.; Cheatham III, T. E. *J. Phys. Chem. B* **2008**, *112*, 9020–9041.
- (8) Li, P.; Roberts, B. P.; Chakravorty, D. K.; Merz, Jr., K. M. *J. Chem. Theory Comput.* **2013**, *9*, 2733–2748.
- (9) Lee, T.-S.; Giambaşu, G. M.; Sosa, C. P.; Martick, M.; Scott, W. G.; York, D. M. *J. Mol. Biol.* **2009**, *388*, 195–206.
- (10) Berendsen, H. J. C.; Grigera, J. R.; Straatsma, T. P. *J. Phys. Chem.* **1987**, *91*, 6269–6271.